

Coupled photonic crystal heterostructure nanocavities

D. O'Brien¹, M.D. Settle¹, T. Karle¹, A. Michaeli², M. Salib³ and
T.F. Krauss¹

¹*Department of Physics and Astronomy, University of St. Andrews, Fife, KY16 9SS, UK*

²*Intel Corporation, Kyriat Gat, 82109, Israel*

³*Intel Corporation, 2200 Mission College Blvd, Santa Clara, CA 95054 USA*

do10@st-andrews.ac.uk

Abstract: We show the first experimental demonstration of multiple heterostructure photonic crystal cavities being coupled together to form a chain of coupled resonators with up to ten cavities. This system allows us to engineer the group velocity of light over a wide range. Devices were fabricated using 193 nm deep UV lithography and standard silicon processing technology. Structures were analysed using both coupled resonator and photonic bandstructure theory, and we highlight the discrepancies arising from subtle imperfections of the fabricated structure.

© 2007 Optical Society of America

OCIS codes: (220.5300) Photonic integrated circuits; (230.0230) Optical devices.

References and links

1. E. Kuramochi, M. Notomi, S. Mitsugi, A. Shinya and T. Tanabe, "Ultra-high-Q photonic crystal nanocavities realized by the local width modulation of a line defect", *Appl. Phys. Lett.* **88**, 041112 (2006).
2. B. S. Song, S. Noda, T. Asano and Y. Akahane, "Ultra-high-Q photonic double heterostructure nanocavity", *Nat. Mater.* **4**, 207-210 (2005).
3. T. A. T. Uesugi, B.S. Song and S. Noda, "Investigation of optical nonlinearities in an ultra-high-Q Si nanocavity in a two-dimensional photonic Crystal slab", *Opt. Express* **14**, 377-386 (2006).
4. A. Yariv, Y. Xu, R. K. Lee and A. Scherer, "Coupled-resonator optical waveguide: a proposal and analysis", *Opt. Lett.* **24**, 711-713 (1999).
5. M. Yanik and S. Fan, "Stopping Light All Optically", *Phys. Rev. Lett.* **92**, 083901 (2004).
6. T. Karle, Y. Chai, C. Morgan, I. White and T. Krauss, "Observation of Pulse Compression in Photonic Crystal Coupled Cavity Waveguides", *IEEE J. Lightwave Technol.* **22**, 514-519 (2004).
7. T. Asano, B. Song and S. Noda, "Analysis of the experimental Q factors (1 million) of photonic crystal nanocavities", *Opt. Express* **14**, 1996-2002 (2006).
8. A. Melloni, F. Moricheti and M. Martinelli, "Linear and nonlinear pulse propagation in coupled resonator slow-wave optical structures", *Opt. Quantum Electron.* **35**, 365-379 (2003).
9. J. B. Khurgin, "Optical buffers based on slow light in electromagnetically induced transparency media and coupled resonators : comparative analysis", *J. Opt. Soc. Am. B* **22**, 1062-1074 (2005).
10. A. Yariv. "Optical Electronics in Modern Communications" (Fifth Edition). Oxford University Press, USA, 1997.
11. S. Johnson and J. Joannopoulos, "Block-iterative frequency-domain methods for Maxwell's equations in planewave", *Opt. Express* **8**, 173-190 (2001).
12. M. Settle, M. Salib, A. Michaeli and T. Krauss, "Low loss silicon on insulator photonic crystal waveguides made by 193nm optical lithography", *Opt. Express* **14**, 2440-2445 (2006).
13. M. Povinelli and S. Fan, "Radiation loss of coupled-resonator waveguides in photonic-crystal slabs", *Appl. Phys. Lett.* **89**, 191114 (2006).

1. Introduction

All optical signal processing remains one of the key goals of photonic systems. Devices that are capable of providing switching functionality and performing logic operations on a stream

of optical bits are one requirement for such a system. The other requirement is an optical buffer that is capable of storing the information while the logic operations are being carried out. Recent developments have shown that photonic crystal nanocavities [1, 2] can provide the strong light-matter interaction required for switching operations [3]. In this paper we show how similar cavities may be used as a solution to the second requirement by providing low dispersion, compact optical delay lines. The interest in photonic crystals for optical buffers or “slow light” applications is largely due to the high degree of control of the optical characteristics that may be achieved by carefully choosing the crystal structure. In a photonic crystal device, a waveguide consisting of a single row of missing holes provides a passband for photons in an otherwise forbidden region of the stop band. This waveguide displays a low gradient dispersion relation close to the spectral cut-off of the passband. The group velocity of light in this region is greatly reduced and the light-matter interaction is enhanced. Unfortunately this slow light region is highly dispersive, making it unsuitable for optical data processing. A coupled resonator structure (CRS), which consists of a series of optical resonators coupled together, has been proposed as a way of slowing the group velocity of light while removing the deleterious effects of dispersion [4]. Similar structures have been suggested for stopping light and storing optical pulses [5]. Previous CRS implementations in photonic crystals have suffered from large losses due to poor vertical confinement along the device [6]. However, recent developments in the area of photonic crystal nanocavities have shown that extremely high Q factors ($Q = 10^6$) may be achieved with very low modal volumes [1, 2, 7]. These structures provide unprecedented control and confinement of photons in both the vertical and lateral directions. We focus on the double heterostructure nanocavity approach [2] for providing the basic element of the CRS. This cavity consists of two different W1 waveguides with slightly different passbands, the optical confinement being provided by this mismatch. The vertical confinement is provided by total internal reflection at the membrane interfaces. By carefully engineering the optical modes in the nanocavity, out of plane losses may be limited while the lateral coupling may be carefully controlled. Devices were fabricated with a number of these cavities in a chain. The cavity resonances in the coupled structure overlap causing a splitting of the optical mode. For a long chain of these cavities, the cavity mode splitting gives rise to a mini passband, providing appreciable bandwidth for slow light operation. The coupling between the cavities affects the overall group velocity of the light, as well as setting the bandwidth of the slow light region. Despite the dramatic improvements in the characteristics of individual cavities, this is the first reported use of these cavities for CRS devices.

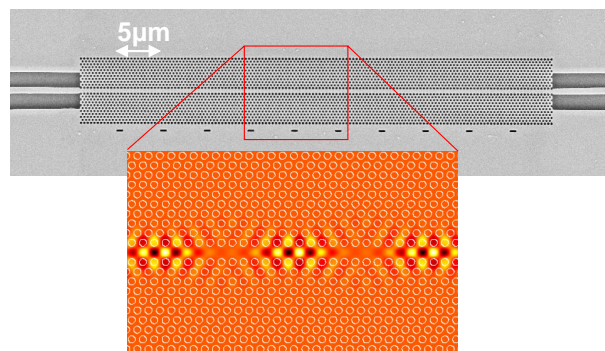


Fig. 1. Scanning electron micrograph image of a chain of 10 coupled heterostructure cavities. The dashed markers below the photonic crystal structure indicate the positions of the lattice shifts that give rise to the heterostructure nanocavities. The electric field profile of the confined cavity modes is shown below for 3 of the cavities.

2. Experiment

The devices were fabricated on silicon on insulator (SOI) wafers with a 240nm Si layer on top of $2\mu\text{m}$ buried oxide (BOX). The pattern was defined using 193nm deep UV lithography and etched using a two-step process. The pattern was first transferred into a hard mask using C_4F_8/O_2 chemistry in a TEL unity etcher and then etched into the Si using Hbr/Cl_2 chemistry in a M511 ECT deep etcher. Finally, a window was defined over the photonic crystal area to selectively remove the SiO_2 layer underneath with HF, while the ridge waveguide remains supported by the unetched SiO_2 . The device design comprises a series of heterostructure cavities [2] separated by 9 rows of holes. The devices had a range of lattice constants around 420nm , which sets the distance between different cavities to $d \sim 5\mu\text{m}$. Different numbers of cavities were coupled together to form the coupled resonator structure (CRS) (see Fig. 1). Chains of 2, 3 and 10 cavities were investigated. Devices were cleaved and then probed using an ASE source with

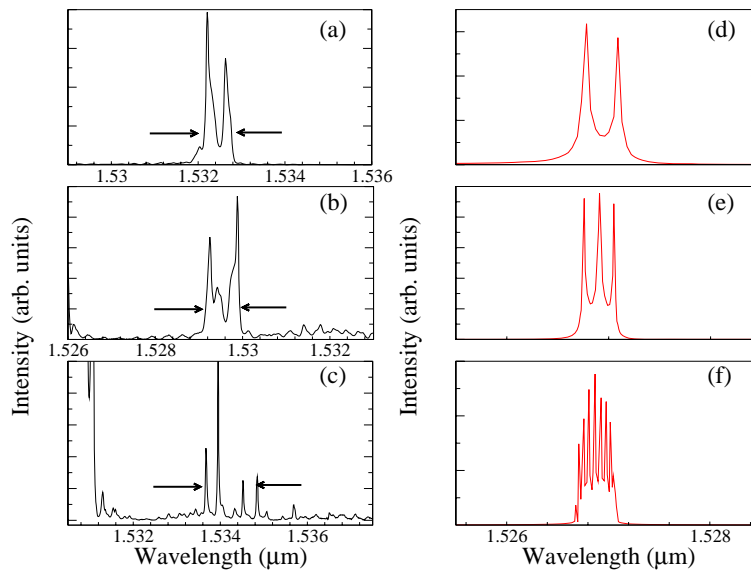


Fig. 2. Left: Experimental transmission spectra for (a) 2 cavity (b) 3 cavity and (c) 10 cavity CRS devices. Arrows indicate the observed 1nm bandwidth. Right: Finite difference time domain (FDTD) calculations of the response of different coupled heterostructure nanocavity systems. (d) Mode splitting observed in 2 coupled cavity, (e) 3 cavity and (f) 10 cavity systems. The bandwidth becomes populated with the additional cavity modes of the chain in the 3 and 10 cavity case. We experimentally observe a small increase in bandwidth for longer chains which we associate with inhomogeneous broadening, caused by small variations in the size of individual cavities. The observed broadening suggests that it will be difficult to achieve a bandwidth below 0.5 nm in such a coupled system. Fabrications tolerances also account for variation in mode amplitudes and positions.

a bandwidth of 50nm in an end fire arrangement along the ridge waveguide. The resulting transmission was collected and analyzed in an optical spectrum analyzer (0.01nm resolution). The linewidth of a single cavity was measured as 0.15nm which corresponds to a Q-factor of 10,000. For the coupled cavity system, a splitting of the optical modes over 1nm was observed. With the addition of further cavities, further mode splitting causes the bandwidth of the defect state to become populated (Fig. 2).

3. Modelling

The measured Q-factor (Q_{meas}) of a single cavity is set by the vertical (Q_{\perp}) and lateral (Q_{\parallel}) quality factors:

$$\frac{1}{Q_{meas}} = \frac{1}{Q_{\perp}} + \frac{1}{Q_{\parallel}}. \quad (1)$$

The lateral Q-factor contributes to the coupling between adjacent cavities, while the vertical Q-factor contributes to losses from the CRS. The relative importance of each component may be calculated by considering the splitting of the optical mode that results from the coupling between multiple cavities in the CRS. Analytically, the dispersion relation for the CRS may be written [8, 9] :

$$\cos(\beta d) = \frac{\sin(kd)}{t}. \quad (2)$$

where β is the phase constant of the propagating wave, t is the transmission coefficient or coupling constant between resonators, $k = \omega n_0/c$ is the wave vector inside each resonator, n_0 being the waveguide linear effective index, and d is the distance between the cavities. The cosine nature of the CRS dispersion relation may be seen in the calculated band diagram of the system (Fig. 3). The outermost frequencies of the defect state satisfy the condition $\sin(kd)/t = 1$. Therefore the bandwidth of the defect state may be defined as :

$$B = \frac{2FSR}{\pi} \sin^{-1}(t). \quad (3)$$

where $FSR = c/2n_0d$ is the free spectral range of the CRS. The bandwidth of the system is set by the transmission coefficient between the cavities t . If t is large, there is good coupling between the cavities and the resulting bandwidth is large. If the coupling between the cavities is decreased, the cavities become more optically isolated from each other and the bandwidth decreases. In the limit of completely decoupled cavities, the bandwidth is set by the Q-factor of an individual cavity. Substituting the observed bandwidth of $1nm$ ($125GHz$) and $FSR = c/2n_0d = 15 THz$ in Eq. 3, we found $t = 0.013$. Using this transmission coefficient and assuming that the lateral losses from individual cavities only arise from coupling into adjacent cavities, the lateral Q-factor may be calculated using [10] :

$$Q_{\parallel} = m \frac{\pi \sqrt{1-t^2}}{t^2}. \quad (4)$$

where we assume a mode order $m = 3$ for the cavity based on the field distribution shown in Ref. [2]. Substituting the value obtained for the transmission coefficient we calculate $Q_{\parallel} = 53,000$. Combining this with the measured Q-factor of 10,000 for an individual cavity, we find $Q_{\perp} = 12,000$ from Eq. 1. These lower than expected values are due to lithographic limitations; while the DUV process ensures excellent reproducibility of adjacent cavities, it is more difficult to ensure accurate fine-tuning of the individual cavities as is required for the ultrahigh Q-factors reported elsewhere [2]. For instance, this specific sample had incorrect optical proximity correction applied, which leads to an increased size of the innermost row of holes. From the slope of the dispersion relation and the observed bandwidth, the group velocity of the mode may be calculated.

$$v_g = \mp \frac{c}{n_0} \frac{\sqrt{t^2 - \sin^2(kd)}}{\cos(kd)}. \quad (5)$$

The slowing factor may then be defined as $S = v/v_g$, which is the ratio of the phase velocity to the group velocity. For the $1nm$ bandwidth observed in the devices tested, this corresponds to a group velocity of $c/140$, and a slowing factor $S = 75$. Bandstructure calculations were performed to check agreement between the above analysis, which applies to any type of coupled resonator system, and the specific photonic crystal system considered here (Fig. 3). The band-

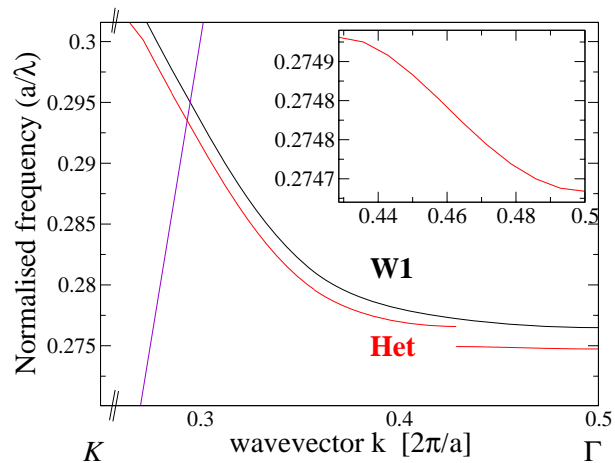


Fig. 3. Band structure of a W1 photonic crystal waveguide alongside a coupled heterostructure waveguide. The defect state associated with the CRS is isolated from the bottom of the waveguide mode. Inset: Close up of the defect state shows that it has a very low group velocity and exhibits very low dispersion for most of the bandwidth of the state. Please note that the bandstructure is simplified and only shows the CRS band for one period of π/d ($0.43 < k [2\pi/a] < 0.5$); in reality, the CRS band repeats with a period of π/d and extends all the way to $k = 0$, thus highlighting the fact that the device operates above the light line.

structure for both a W1 photonic crystal waveguide and a CRS were calculated using the MIT photonic bands (mpb) software [11]. The chain of heterostructure nanocavities can be viewed as a periodic perturbation on the standard W1 photonic crystal waveguide, which causes a discontinuity in the band corresponding to the CRS mode. The CRS modes operate past the spectral cutoff of part of the waveguide. This part of the waveguide acts as a mirror and defines the cavities, transmission along the CRS occurring through evanescent mode coupling from one cavity to the next. The appearance and properties of this mode may be altered by changing the inter-cavity coupling constant either by varying the number of rows of holes separating the cavities during fabrication, or by dynamically detuning individual cavities via thermal or carrier effects. When modelling the measured system, i.e. a heterostructure comprised of mirrors with 9 rows of holes, the bandwidth was lower than observed experimentally. This is also seen in the FDTD calculations that exhibit a bandwidth of $0.5nm$ as opposed to the experimentally observed $1nm$ (Fig. 2). Reducing the mirror size from 9 to 4 rows of holes allowed us to match the bandwidth with that observed. This suggests that a degree of disorder is present in the mirror which reduces its effective reflectivity. It seems curious that the low disorder in the photonic crystal that we observe otherwise (around $1 - 2nm$ RMS deviation in hole position and hole radius by SEM analysis [12]) should have such a large impact, but it indicates that the relatively subtle confinement mechanism of the photonic crystal heterostructure is very sensitive to disorder.

In order to explore the limits of this system, assuming that the sources of loss may be limited, we take the ideal case where $Q_{meas} = Q_{||}$. In this case, all of the light that escapes from an individual cavity is coupled to its neighbours (Fig. 4). Given that a single cavity $Q = 10^6$ has

already been demonstrated with much higher values already predicted ($Q = 2 \cdot 10^7$) [2], slowing factors greater than 300 may be achieved by coupling such cavities together. In this limit of very high Q factor, however, fabrication tolerances may prevent keeping a chain of cavities close to resonance with one another. As we have shown here, even the smallest inaccuracies introduced by State-of-the-Art fabrication technology already have an impact on the subtle confinement mechanism in photonic heterostructure cavities. Assuming, therefore, a practical bandwidth limit of 0.5nm , it would still be possible to use a $700\mu\text{m}$ long device consisting of ~ 140 nanocavities as a $> 1\text{ns}$ delay line. For such a device, we estimate an upper bound of 6dB/ns from the individual Q and point to the fact that the real losses may be lower [13].

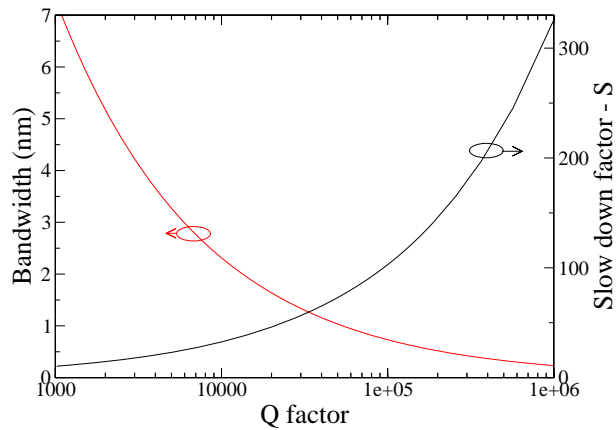


Fig. 4. For the ideal case where losses are negligible, the relationship between the bandwidth of the defect state B , slowing factor S and the individual cavity Q-factor is calculated.

Due to the strong light matter interaction brought about by the low mode volume, high Q optical cavity, non-linear behavior can also be observed using these photonic crystal nanocavity structures at relatively low power levels [3]. These non-linear effects could also be harnessed for changing the behavior of the array of cavities. If the array was to function as an optical delay line, the delay time could be dynamically tuned by detuning individual cavity resonances, as proposed by Fan [5].

4. Conclusions

In summary, we have shown the first demonstration of a coupled resonator system based on as many as 10 photonic crystal heterostructure nanocavities. The coupled system exhibits a bandwidth of approximately 1 nm at 1550 nm with a corresponding group velocity of $v_g=c/140$ and slowing factor of $S = 75$. Although we find that some degree of disorder must be present in order to explain the lower than expected mirror reflectivity, the fact that the bandwidth of the system has little dependence on the number of cavities suggests that the variation of the individual cavity resonances is smaller than the bandwidth of the system. The disorder in the photonic crystal is at the present state of the art ($\sim 1\text{nm}$ variation in hole size and position) and our data suggests that it will be difficult to achieve bandwidths below 0.5nm , even for perfectly designed cavities. Assuming this bandwidth, a delay line for inducing a delay of 1 ns would require a chain of 140 cavities. For such a device, we estimate an upper bound of 6dB/ns from the ringdown time of an individual cavity of $Q = 10^6$, although the real losses in the coupled system may be lower.

The research in this paper was funded through a three-year Strategic Research grant from Intel Corporation.